

View of the empty states of the Si(100)-(2×1) surface via scanning tunneling microscopy imaging at very low biases

X. R. Qin and M. G. Lagally

University of Wisconsin-Madison, Madison, Wisconsin 53706

(Received 29 September 1998)

It is shown that the use of very-low-bias voltages in scanning tunneling microscopy of the Si(100)-2×1 surface achieves significantly greater sensitivity to the electronic states of the top atomic layer than does the use of typical larger bias voltages. Measurements with the increased sensitivity demonstrate that the conventional interpretation of empty-state images of Si(100) is inadequate. New spectroscopic assignments for observed features are proposed. [S0163-1829(99)05708-2]

Scanning tunneling microscopy (STM) has provided many breakthroughs in imaging surfaces on the atomic scale.¹ Some of the most notable of these have been for the Si(100) surface, which has great technological importance and also serves as the model semiconductor system for studying atomistic growth mechanisms² and electronic properties. Filled-state imaging, for which electrons tunnel from the surface into the STM tip, has been conventionally used for mapping the surface morphology and structure. Because Si has a significant density of states^{3,4} within the probing energy window, filled-state images lead to a strong tunneling signal. Empty-state imaging, with electrons tunneling from the tip into the surface, has recently attracted interest for identifying local electronic states, because empty-state images are more sensitive to dangling-bond orbitals associated with adsorbed atoms.⁵⁻⁸ However empty-state imaging of Si(100), which should be background knowledge for investigations of adsorbed-atom electronic properties, has not been fully enough explored to provide a consistent and physically realistic picture of the empty states of the clean surface.

As is well known, the Si(100)-2×1 surface, in order to reduce surface energy, reconstructs to form rows of tilted dimers:⁹⁻¹¹ the two atoms of a dimer are positioned up and down relative to the surface plane. The dimer formation leaves one dangling bond per surface atom, and the two dangling bonds of a dimer form a π -like bonding to stabilize the surface structure further.^{12,13} The conventional empty-state STM image of the Si(100) surface has a minimum in the tunneling current at the center of the dimer bond, making the tops of the dimer rows appear as dark bands, while tunneling maxima occur between the dimer rows.^{3,12,13} A popular interpretation of these features is based on the concept that the π -like bonding of the two atoms of the dimer dominates the electronic behavior in the empty-state imaging:^{3,13} because the unoccupied antibonding π state (i.e., the π^* state) has a node^{10,14} in the middle of the dimer bond, the state density there drops to zero, resulting in an image that shows well-resolved “atoms” in the dimer. This π^* description has been widely used. There are, however, two concerns. First, conventional empty-state images do not show the tilting (buckling) of dimers even when these are pinned or adjacent to defects, in disagreement with the π^* state density

calculations.^{10,14} Second, theories¹⁴⁻¹⁶ show that the antibonding dimer-bond (σ^*) level is near the bottom of the conduction band. It has been suggested that the σ^* state might be energetically accessible in addition to the π^* dangling bonds.¹² As the σ^* state has a maximum state density at the ends of the dimer, it could presumably also be responsible for the empty-state STM image.

The interpretation of the conventional empty-state image of Si(100) is therefore still ambiguous; measurements have been of insufficient quality and detail to resolve the ambiguities. In this Brief Report, we show, on the basis of very-low-bias high-resolution STM studies, that the conventional understanding of empty-state imaging of the Si(100)-2×1 surface is inadequate. We revise the interpretation, and explain why the surface sensitivity is greatly enhanced in our experiment.

The experiments were carried out in an ultrahigh-vacuum scanning tunneling microscope with a base pressure below 1×10^{-10} Torr. The clean Si(100)-2×1 surface was prepared in the conventional manner¹⁷ by degassing at 970 K and flashing at 1470 K for ~ 1 min. The sample was radiation cooled, then transferred to the STM stage and imaged at room temperature. All images were acquired in the constant-current mode using a tunneling current of 0.2 nA.

Figure 1 shows the same region of a Si(100) surface at different biases. Figure 1(a) shows the well-known filled-state image. The long bands running through the diagonal of the frames are the Si dimer rows, in which individual dimers are clearly resolved. Dimers away from defects appear symmetric, with a “bean” shape. This is because a tilted dimer has two possible orientations of the tilt that are energetically equivalent, and the kinetic barrier for moving from one to the other is low; at room temperature, on the time scale of typical STM image acquisition, the tilted dimers are oscillating (“dynamic buckling”), due to thermal activation, between the two equivalent positions, causing the average symmetric appearance.^{3,11} Figure 1(a) also shows that dimers adjacent to a surface defect are statically “buckled” (smaller zigzag protrusions along the dimer rows, such as in the area between the two black lines marked by arrows), because atomic defects can induce or stabilize the buckling.^{3,11}

Figures 1(b)–1(h) show a set of empty-state images of the same surface area under different sample biases. At high

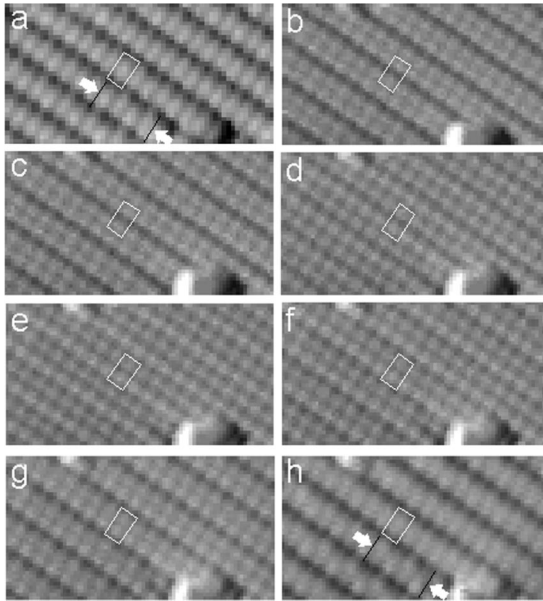


FIG. 1. Scanning tunneling microscope images of the Si(100)- 2×1 surface. (a) Filled-state image. (b)–(h) A set of empty-state images of the same area at different sample biases. The rectangle shows the same Si dimer in each image. The zigzag patterns marked by arrows in (a) and (h) show buckled dimers at the same location: the two zigzag patterns have opposite phases. Sample biases: (a)–(h) -2 V, $+2$ V, $+1.8$ V, $+1.6$ V, $+1.4$ V, $+1.1$ V, $+1.0$ V, and $+0.7$ V. Image size: 65×30 Å².

bias, $+2$ V, the image [the rectangle in Fig. 1(b)] shows characteristics of a conventional empty-state image of the surface: a deep minimum between the two Si atoms forming the dimer bond and a shallow minimum between dimer rows, which is usually observable with a sharp tip. These features are maintained to biases of about $+1.4$ V [Figs. 1(b)–1(e)]. With decreasing sample bias, the difference between the deep minimum and the shallow minimum becomes smaller, until at about $+1.1$ V [Fig. 1(f)], a reversal of the contrast occurs. At lower biases, new features are immediately obvious. For example, at $+0.7$ V [Fig. 1(h)], the tunneling maxima again conform to the dimer bond locations, with the same image registration as that of the filled-state image [Fig. 1(a)]. The dimers not only appear symmetric but also “bean” shaped; Fig. 1(h) could easily be taken for a filled-state image. Second, in contrast to empty-state images at higher bias voltage, in which dimer buckling is essentially invisible, buckled dimers clearly stand out from beans in Fig. 1(h). However, the zigzag pattern of the buckling is out of phase with that in the filled-state image [Fig. 1(a)]. These low-bias imaging properties are maintained up to ~ 0.8 V, and a hint of these features appears up to biases of ~ 1.0 V [Fig. 1(g)]. The dramatic differences in the dimer image in the empty-state tunneling contour between conventional high bias (H contour) and the low bias (L contour) are shown schematically in Fig. 2.

The low-bias image [e.g., Fig. 1(h)] clearly suggests that the conventional view of the empty-state image of the Si(100)- 2×1 surface is incomplete and inadequate: (1) the fact that the static buckling is invisible in high-bias images but visible in low-bias images indicates that the high-bias images cannot be explained by the surface π^* state; and (2)

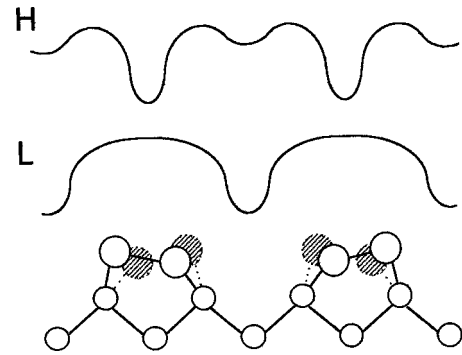


FIG. 2. Schematic STM empty-state imaging contours at high-bias (H) and low-bias (L) conditions, and their relationship to the underlying dimers, which at room temperature oscillate between two buckling configurations (solid and shaded).

the conventional π^* description, which requires a node at the middle of the dimer bond, cannot explain the bean-shaped dimers at the low bias.

We believe that the low-bias image more properly reflects the unoccupied dangling-bond (π^*) state. First, low-bias imaging is energetically more focused on the π^* state. Scanning tunneling spectroscopy empty-state spectra⁴ of a dimer consist of a weak peak at ~ 0.5 eV and a strong peak at ~ 1.5 eV above the Fermi energy E_f . The former corresponds to the π^* state.⁴ The latter has never been clearly interpreted, but it is located at an energy at which the combination of antibonding states associated with the dimer bond (σ^*) and backbond is proposed to occur.¹⁵ It has been suggested that the backbond decays rapidly with distance from the surface,¹⁴ if its antibonding state also behaves so, then the 1.5-eV peak is more likely attributable to the σ^* state weighting. In any case, because only states between E_f and $(E_f + eV)$ contribute to the tunneling process, high-bias (e.g., $+2.0$ V) imaging probes states at both $+0.5$ and $+1.5$ eV, whereas low-bias (e.g., $+0.7$ V) imaging cannot probe states at $+1.5$ eV. Second, in contrast to high-bias imaging, in which dimer buckling is essentially invisible, low-bias imaging not only shows the buckling, but shows it as a mirror image of that seen with a bias of the reverse sign [Fig. 1(a)]. It is well accepted that the “up” atom of the tilted dimer appears brighter in filled-state images. The mirror image obtained in the low-bias empty-state imaging suggests that the “down” atoms of the tilted dimers are now more visible. These results are fully in agreement with the π^* state density calculations:^{10,14} the two atoms of the dimer should have different state densities, with the down atom having the higher empty-state density, and with the up atom having the higher filled-state density.

From the above analysis, we conclude that the conventional high-bias empty-state images are not predominantly determined by the surface dangling-bond state, but instead mainly by other states. The insensitivity, at high biases, to buckling is because the images do not have an effective contrast of the dangling-bond state over the background contributions from other states. Our results on the buckling also demonstrate that the low-bias imaging is dominated by surface electronic structure rather than by geometric structure.

If the buckling results confirm the role of the π^* state in the density of local empty states on Si(100), how can one

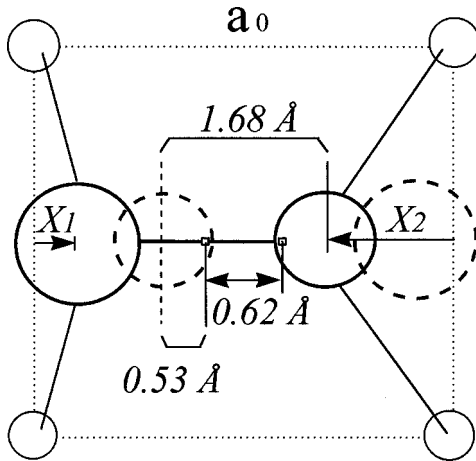


FIG. 3. Top view of an intrinsically buckled dimer. The circle size represents the height. The dotted frame is the 1×1 bulk unit mesh with lattice constant, $a_0 = 3.84 \text{ \AA}$. The two dimer atoms are displaced from the 1×1 bulk positions by $x_1 = 0.46 \text{ \AA}$ and $x_2 = -1.08 \text{ \AA}$ (Ref. 10), respectively. The alternative buckling configurations are shown by solid and dashed circles. The projected center of gravity for the dimer in the configuration indicated by solid circles is 0.62 \AA away from that indicated by dashed circles, and 0.53 \AA away from the center of the “down” atom in the configuration indicated by the dashed circles. The distance between down atoms in the two configurations is 1.68 \AA .

explain the bean-shaped dimers in the low-bias images? We propose that the bean-shaped Si dimers [Fig. 1(h)] arise because the node of the π^* state is shifted when the dimer oscillates and is smeared out when the STM measurement averages the motion. The dimer tilting is always accompanied by two effects: charge transfer from the lower dimer atom to the upper one, and the displacement of the dimer center of gravity (projected into the plane of the unbuckled dimer) along the dimer axis.¹⁰ Charge transfer leads to a polarization of the π bond,¹⁰ the polarization shifts the node of the π^* state from the center of the dimer bond along the dimer axis. The node shift will be enhanced because the two atoms in a buckled dimer are asymmetrically displaced from the 1×1 bulk positions.^{10,18} Therefore, although there is a node in the polarized π^* state, oscillation of buckled dimers shifts the node back and forth, and thus may smear it out, leading to the observation of bean-shaped dimers in the image. Qualitatively, the larger the tilt angle, the greater is the node shifting, and the stronger is the smearing-out effect when the dimer oscillates.

We quantitatively analyze the case of an intrinsically buckled dimer using the available calculated results¹⁰ in the

literature. We first estimate the range for the node shifting. The atomic positions for the dimer atoms are shown in Fig. 3. The dimer center of gravity projected into the plane of the unbuckled dimer is then deduced to be offset by 0.31 \AA . Dynamic buckling leads to the projected dimer center of gravity moving in a range of 0.62 \AA , more than 27% of the dimer bond length ($\sim 2.30 \text{ \AA}$). STM measures a time average over all different tilting angles between the two intrinsic buckling configurations. The two extreme positions (Fig. 3) are expected to be highly weighted in the average because they are the lowest-energy states and thus the most stable configurations. We thus consider the relative positions of the two configurations in order to understand the node smearing-out effect in the time-average measurement. The distance between the down atoms in the two configurations is 1.68 \AA , which is significantly less than the dimer bond length. As already mentioned, the down atom appears brighter in the low-bias STM image, thus we see approximately the “time lapse photograph” of a “bright” atom moving in this short distance. Furthermore, the shifted π^* node in one configuration (solid circles in Fig. 3) is very close to the bright down atom in the opposite configuration, with a 0.53-\AA separation (or less, as charge-transfer effects have not been included). Therefore, the shifted node can also be effectively weakened in the time-average sense, leading to the bean-shaped dimer image.

Our interpretation for the beans is also consistent with low-temperature STM observations.¹⁹ Because dynamic buckling is inhibited at low temperatures, all the dimers are buckled, smearing-out effects are absent, and no beans are observed in the empty-state imaging.

Because low-bias imaging of the empty states shows great enhancement of the STM sensitivity to the surface states (Fig. 4), a greater sensitivity to structural information is also obtained. At room temperature, low-bias imaging of Si(100) allows us to locate dynamically buckled dimers (which appear as beans), to find the statically buckled dimers (which have their down ends more visible), and to identify less tilted dimers or symmetric dimers [which should have a well-defined node or minimum at the center of the dimer bond, e.g., the arrow in Fig. 4(c)]. None of these identifications can be made in the conventional high-bias empty-state images. The last one is also not possible in filled-state imaging [e.g., the arrow in Fig. 4(a)], because the π bonding state does not have a node; hence dynamic dimer buckling makes an intrinsically buckled dimer appear the same in the filled-state images as a symmetric dimer. We have successfully applied the low-bias imaging approach to reveal the local buckling variation in the vicinity of Ge or Si ad-dimer is-



FIG. 4. Sensitivity of STM images of Si(100) to bias voltage. A filled-state image (a) [-2.0 V] and two empty-state images taken with sample biases of (b) $+2.0 \text{ V}$ and (c) $+0.8 \text{ V}$. White frames show the same area. Arrows point to an identical dimer in the vicinity of a missing-dimer defect; the dimer appears symmetric and can only be distinguished from others in (c). Image size: $85 \times 65 \text{ \AA}^2$.

lands. The strain field induced by the ad-dimer islands pins the dimers in much less buckled configurations than that for an intrinsically buckled one.²⁰

In summary, using STM measurements at a variety of very low biases, we show that the conventional understanding of the empty-state imaging of the Si(100)- 2×1 surface is inadequate. We show that the low-bias images dominantly reflect the surface dangling-bond state, while the conventional high-bias images reflect mixed states, with the surface state contribution not prominent. We demonstrate an enhancement of the STM sensitivity to the surface states at low biases that other bias conditions cannot achieve, with the

added result that we are able to distinguish structural configurations of the Si dimers that are not obtainable at conventional biases. We believe these results enhance the understanding of the clean-surface electronic structure that is necessary for considering the electronic properties of more complex adsorbed-atom systems.

Note added in proof. We recently became aware of similar work, as yet unpublished, by K. Hata, S. Yasuda, and H. Shigekawa, Phys. Rev. B.

This work was supported by NSF (Grant No. DMR93-04912) and by Sandia National Laboratories (Grant No. AS-1168).

-
- ¹G. Binnig, H. Rohrer, C. Gerber, and E. Weibel, Phys. Rev. Lett. **50**, 120 (1983).
- ²For a review and an extended list of references, see Zhenyu Zhang, and M. G. Lagally, Science **276**, 377 (1997).
- ³R. J. Hamers, Ph. Avouris, and F. Bozso, Phys. Rev. Lett. **59**, 2071 (1987); J. Vac. Sci. Technol. A **6**, 508 (1988).
- ⁴J. J. Boland, Phys. Rev. Lett. **67**, 1539 (1991).
- ⁵P. J. Bedrossian, Phys. Rev. Lett. **74**, 3648 (1995).
- ⁶G. Brocks and P. J. Kelly, Phys. Rev. Lett. **76**, 2362 (1996).
- ⁷B. S. Swartzentruber, Phys. Rev. B **55**, 1322 (1997).
- ⁸X. R. Qin and M. G. Lagally, Science **278**, 1444 (1997).
- ⁹F. J. Himpsel and Th. Fauster, J. Vac. Sci. Technol. A **2**, 815 (1984).
- ¹⁰D. J. Chadi, Phys. Rev. Lett. **43**, 43 (1979); J. Ihm, M. L. Cohen, and D. J. Chadi, Phys. Rev. B **21**, 4592 (1980).
- ¹¹R. A. Wolkow, Phys. Rev. Lett. **68**, 2636 (1992).
- ¹²*Scanning Tunneling Microscopy*, edited by J. A. Stroscio and W. J. Kaiser (Academic, New York, 1993).
- ¹³J. A. Kubby and J. J. Boland, Surf. Sci. Rep. **26**, 61 (1996).
- ¹⁴J. Pollmann, P. Kruger, and A. Mazur, J. Vac. Sci. Technol. B **5**, 945 (1987).
- ¹⁵S. Ciraci, R. Butz, E. M. Oellig, and H. Wagner, Phys. Rev. B **30**, 711 (1984).
- ¹⁶P. Kruger, A. Mazur, J. Pollmann, and G. Wollgarten, Phys. Rev. Lett. **57**, 1468 (1986).
- ¹⁷B. S. Swartzentruber, Y.-W. Mo, M. B. Webb, and M. G. Lagally, J. Vac. Sci. Technol. A **7**, 2901 (1989).
- ¹⁸A. Garcia and J. E. Northrup, Phys. Rev. B **48**, 17 350 (1993).
- ¹⁹D. Badt, H. Wengeinik, and H. Neddermeyer, J. Vac. Sci. Technol. B **12**, 2015 (1994).
- ²⁰X. R. Qin, Feng Liu, B. S. Swartzentruber, and M. G. Lagally, Phys. Rev. Lett. **81**, 2288 (1998).